Lifetimes of states in the opposite-parity bands of ^{153}Eu: Recoil-distance measurements following Coulomb excitation

J. F. Smith,[1,*] M. W. Simon,[2] R. W. Ibbotson,[2,†] P. A. Butler,[1] A. Aprahamian,[3] A. M. Bruce,[4] D. Cline,[2] M. Devlin,[2,‡] G. D. Jones,[1] P. M. Jones,[1,§] and C. Y. Wu[2]

[1]*Oliver Lodge Laboratory, University of Liverpool, Liverpool, L69 3BX, United Kingdom*

[2]*Nuclear Structure Research Laboratory, University of Rochester, Rochester, New York 14627*

[3]*Physics Department, University of Notre Dame, Notre Dame, Indiana 46556*

[4]*Department of Mechanical and Manufacturing Engineering, University of Brighton, Brighton, BN2 4GJ, United Kingdom*

(Received 19 March 1998)

The lifetimes of 12 states in the opposite-parity bands of ^{153}Eu have been measured using a recoil-distance technique following Coulomb excitation with a 220-MeV ^{58}Ni beam. Electric-quadrupole (Q_0) and -dipole (D_0) moments, and intrinsic g factors (g_K) have been extracted from the lifetimes. The Q_0 and D_0 values show very little dependence on spin and parity, and have the values of approximately 6.6 e b and 0.077 e fm, respectively. The g_K values are found to differ for the positive- and negative-parity states. Although the large D_0 values suggest a reflection-asymmetric octupole-deformed nuclear shape, the different g_K values contradict this interpretation. A discussion of the nuclear structure of ^{153}Eu in terms of potential parity-doublet bands and octupole deformation is given. [S0556-2813(98)02511-4]

PACS number(s): 21.10.Ky, 21.10.Tg, 23.20.Lv, 27.70.+q

I. INTRODUCTION

Near-degenerate states with equal spin and opposite parity, known as parity doublets, are one of the experimental characteristics of octupole deformation in odd-mass nuclei [1–4]. Rotational bands with very similar properties may be built upon the parity-doublet states. Within such bands, the intrinsic gyromagnetic ratios g_K will therefore be the same for the states with I^+ and I^-. Furthermore, as a consequence of the octupole-deformed shape, enhanced electric-dipole transitions may be observed, connecting the states with spin and parity $I^{+/-}$ to those with $(I-1)^{-/+}$. Several examples of parity-doublet bands have been observed in nuclei in the light-actinide region; one of the best cases is that of $^{223}_{90}$Th [5], and similar structures have also been seen in ^{225}Th [6], $^{221}_{88}$Ra [7], and $^{220}_{89}$Ac [8]. In the rare-earth region where octupole correlations are weaker [9,10], bands have been observed in some odd-proton nuclei such as $^{151}_{61}$Pm [11,12] and $^{153}_{63}$Eu [13], which have all the characteristics of parity-doublet partners. However, these nuclei lie away from the predicted center of octupole deformation in this region ($^{146}_{56}$Ba$_{90}$) and some recent studies [14] have suggested that the suspected parity-doublet bands can be explained without invoking octupole deformation.

The stable isotope ^{153}Eu is the subject of the present work. This nucleus has previously been studied by Coulomb excitation: Lewis and Graetzer [15] first observed states up to $9/2^+$, and the level scheme was extended to $15/2^+$ by Thun and Miller [16]. Dracoulis *et al.* [17] used the ^{154}Sm(d,3n) reaction, and arranged the excited states into rotational bands. In the most recent study, Pearson *et al.* [13] used the ^{150}Nd(^{7}Li,4n) reaction. Part of the level scheme deduced in that work is shown in Fig. 1. The levels may be arranged in sequences which have the characteristics of parity-doublet bands. Furthermore, electric-dipole moments (D_0) and g factors (g_K-g_R) were inferred from the measured $B(E1)/B(E2)$ and $B(M1)/B(E2)$ ratios. States in the opposite-parity bands were found to have large, collective D_0 values, suggestive of octupole correlations, but (g_K-g_R) values were found to be different for the states of different parity, implying that the bands are not based on an intrinsic parity-mixed state. A more recent high-spin study by Basu *et al.* [18] has presented some evidence that the (g_K-g_R) values may become equal in the positive- and negative-parity bands at high spin, although large errors in the data points make their work rather inconclusive. The conclusions of Ref. [13] were based on the assumption of a constant quadrupole moment within the opposite-parity bands, equal to the measured spectroscopic quadrupole moment of the ground state [19]. A measurement of the lifetimes together with experimental branching ratios allows electromagnetic moments and absolute $B(E2)$, $B(M1)$, and $B(E1)$ values to be determined from which nuclear-structure information can be deduced without such assumptions.

The goal of the present work was to measure the lifetimes in the opposite-parity bands of ^{153}Eu. Prior to this work, only the lifetimes of the $7/2^+$, $9/2^+$, $5/2^-$, and $7/2^-$ states had been measured [16]. In this work the lifetimes of the $9/2^+$ to $25/2^+$ states in the positive-parity band (nine states) and $17/2^-$ to $21/2^-$ states in the negative-parity band (three states) have been measured.

*Author to whom correspondence should be addressed. Present address: Schuster Laboratory, University of Manchester, Manchester, M13 9PL United Kingdom. Fax: (44) 161 275 5509. Electronic address: jfs@mags.ph.man.ac.uk

†Present address: National Superconducting Cyclotron Laboratory, Michigan State University, East Lansing, Michigan 48824.

‡Present address: Chemistry Department, Washington University, St. Louis, Missouri 63130.

§Present address: Department of Physics, University of Jyväskylä, Jyväskylä, FIN-40351, Finland.

 ©1998 The American Physical Society

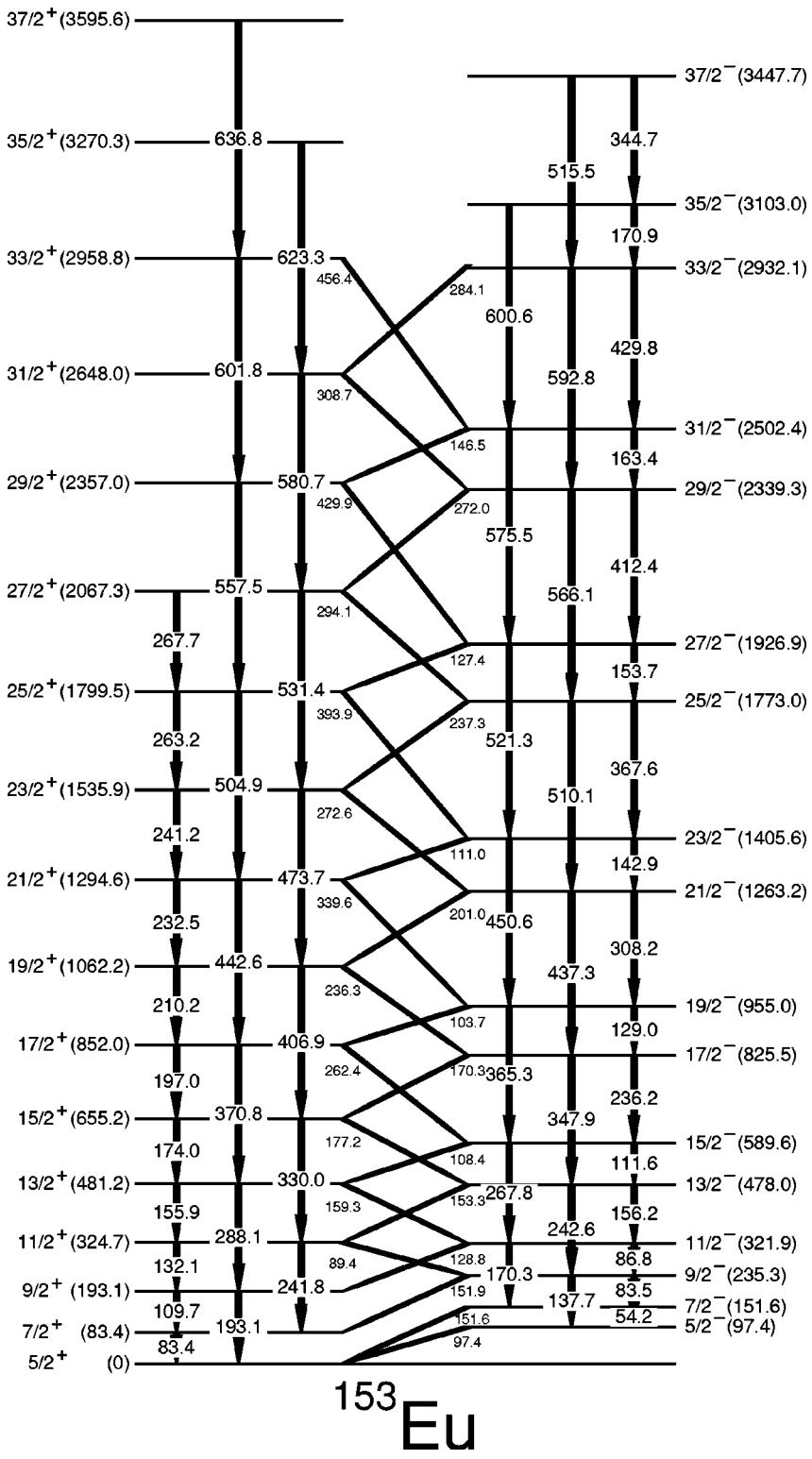

FIG. 1. The levels in ^{153}Eu observed in this work.

II. EXPERIMENTAL DETAILS

Since simple rotational-model estimates suggest that the lifetimes of interest should be of the order 10^{-9}–10^{-12} s, a recoil-distance method was chosen for the measurement. The particular recoil-distance technique that was used has been described in earlier publications [20,21]; a schematic depiction of the apparatus is shown in Figure 2. Excited states in ^{153}Eu were populated using Coulomb excitation, primarily because this allows the populations of the states to be calculated exactly, and hence allows correction for feeding from higher-lying states to be made when extracting the lifetimes. A thin target of ^{153}Eu was bombarded with a 220-MeV ^{58}Ni beam from the Rochester 16 MV MP tandem Van de Graaff accelerator. The beam energy was at ~80 % of the Coulomb

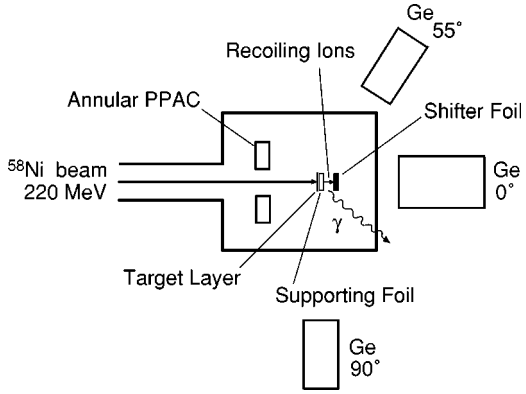

FIG. 2. Arrangement of the Rochester recoil-distance apparatus. The detector at 0° has an efficiency of 70%, relative to that of a 3 in. × 3 in. NaI(Tl) detector, while the other two detectors have an efficiency of 20%. The detectors at 0°, 55°, and 90° are positioned at 120 mm, 150 mm, and 200 mm from the target, respectively.

barrier, in order to ensure that the excitation was purely electromagnetic. The target consisted of approximately 390 μg/cm^2 of 99%-enriched ^{153}Eu, evaporated onto a 500 μg/cm^2 ^{58}Ni backing. Three Compton-suppressed germanium detectors were used, the details of which are given in Fig. 2. Gamma rays were collected in coincidence with backscattered ^{58}Ni ions, which were detected by an annular parallel-plate avalanche counter (PPAC) filled with isobutane at a pressure of 4 Torr [22]. The PPAC was placed 54 mm upstream of the target and covered an angular range of 138°–168° with respect to the beam direction. This corresponded to the target nuclei recoiling into a forward-focused cone covering approximately 4°–13°.

The recoil-distance method used was a variation of the standard method. Instead of stopping the recoils in a ''stopper'' foil, a 2.8-mg/cm^2 nickel ''shifter'' foil was placed downstream of the target in order to reduce the speed of the recoiling target nuclei. The difference in Doppler-shifted gamma-ray energies from nuclei deexciting before the shifter foil (with full recoil velocity) and after the shifter foil (with reduced velocity) was found to be about 9 keV at a gamma-ray energy of about 500 keV. The shifter foil was aligned to within 0.6° of the orientation of the target by reflecting the beam of a He-Ne laser from the surface of both the target and the shifter foil [20]. An ''Inchworm'' transducer device, manufactured by Burleigh Instruments, Inc., was used to move the shifter foil in 6-nm steps, over a range of about 25.4 mm. For small distances the target-to-shifter foil distance d was determined by measuring the capacitance between the target and shifter foil, which varies in inverse-proportion to d [23]. For large distances an optical encoder was used to determine the separation to an accuracy of $\sim$2 μm.

In total, data were recorded for 14 recoil distances. The distances used in μm were 16, 24, 38, 62, 100($\times$2), 200, 320, 450, 800, 1500, 3000, 5000, 8000, and 10 000. Data were collected for almost 24 h for several of the shorter distances, to ensure that enough events were collected to measure the shortest lifetimes of the highest levels. The recoil velocity had to be determined in order to extract the lifetimes. This was measured by replacing the shifter foil with a thick 11-mg/cm^2 nickel foil in which the recoils were brought to rest. A measurement of the energy difference between the stopped peaks (with no Doppler shift) and the *fast* peaks (with the full Doppler shift) for the strongest transitions enabled the velocity to be calculated. The gamma rays were detected at 0° and a correction was made for the finite solid-angle subtended by the germanium crystal. The recoil velocity between the target and the shifter foil was found to be $v/c=0.0435(7)$, and this was reduced to $v/c=0.0257(4)$ after the shifter foil.

III. ANALYSIS

The procedure for extraction of the lifetime from recoil-distance data is given in many references such as [24]. In essence, the method involves construction of the ratio R, where

$$R=\frac{I_s}{I_s+I_f}, \tag{1}$$

and I_s and I_f are the intensities of the ''slow'' (small Doppler shift) and ''fast'' (large Doppler shift) peaks, respectively. As a first-order approximation it can be assumed that the decay of the states is purely exponential, that is,

$$\ln R=\frac{-d}{v\tau}, \tag{2}$$

where v is the recoil velocity, d is the recoil distance (between the target and the shifter foil), and τ is the lifetime of the state. The peak intensities I_s and I_f were measured using the spectrum-analysis code GF2 from the RADWARE [25] series of analysis codes.

There are several effects which perturb the simple linear relationship of Eq. (2) and will alter the experimentally measured intensities. In brief, these are (i) relativistic solid-angle effects, (ii) geometric solid-angle effects, (iii) energy-dependent detector efficiencies, (iv) finite detector size, (v) the nuclear-deorientation effect, (vi) feeding from higher-lying states, and (vii) gamma-ray emission during passage through the shifter foil. Corrections had to be made for these perturbing effects and these were carried out using a version of the code ORACLE [26]: the original code was modified [27] to compute time-ordered decay, in order to account for complicated branching of gamma decay, which is necessary for treating odd-A nuclei. The perturbations caused by the nuclear deorientation effect were corrected using the two-state model [28] with parameters that have been found to fit a wide range of nuclei [29].

The Rochester Coulomb-excitation code GOSIA [30] was used to calculate the populations of the states in order to correct for feeding. To calculate the excitation probabilities, GOSIA requires the electromagnetic transition matrix elements for all the significant couplings. In calculating the feeding correction, a several-step iterative process was used. As an initial estimate matrix elements were calculated using rotor-model equations (given below). These matrix elements were then used by the code GOSIA to compute the Coulomb-excitation probabilities for each level, from which the feeding correction was calculated. The calculated intensities were then used to extract lifetimes and hence experimental matrix elements, using the procedure described above. The experi-

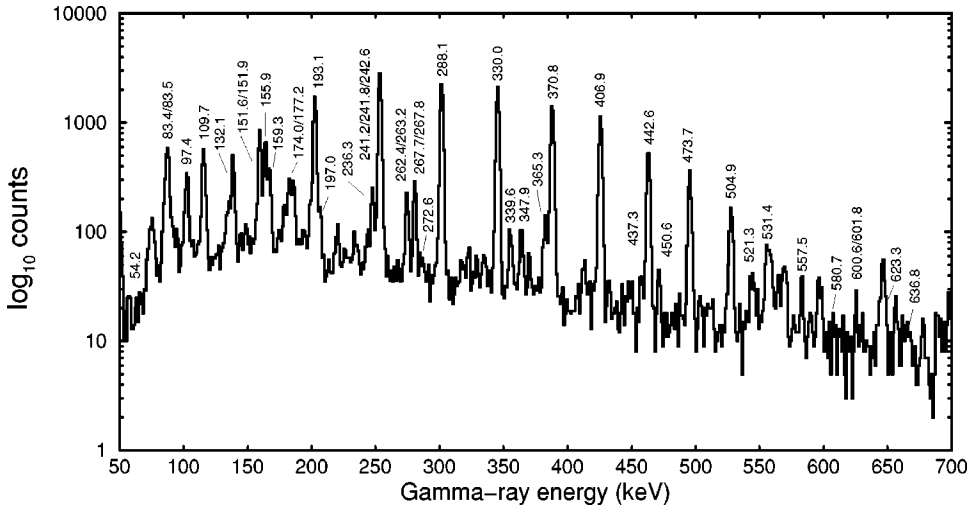

FIG. 3. Summed spectra for recoil distances $d=8000$ μm and $d=10\,000$ μm, recorded by the large-volume germanium detector at 0°. The intensity at such long recoil distances lies predominantly in the the fully Doppler-shifted (fast) peaks. The peaks are marked with the unshifted gamma-ray energies.

mental matrix elements were then input into GOSIA which calculated an improved feeding correction, which was in turn used to extract more accurate experimental matrix elements. This iterative process was found to converge rapidly. The initial set of rotor-model matrix elements was calculated using the rotor-model equations

$$\langle I_i||E\lambda||I_f\rangle=\sqrt{(2I_i+1)}a_\lambda Q_{\lambda 0}\langle I_iK_i\lambda 0|I_fK_f\rangle, \tag{3}$$

$$\langle I_i||M1||I_f\rangle=\sqrt{(2I_i+1)}\sqrt{\frac{3}{4\pi}}(g_K-g_R)K_i\langle I_iK_i10|I_fK_f\rangle, \tag{4}$$

$$a_{\lambda\neq 1}=\sqrt{\frac{2\lambda+1}{16\pi}},\quad a_1=\sqrt{\frac{3}{4\pi}}, \tag{5}$$

where g_K and g_R are the intrinsic and rotational gyromagnetic ratios and $Q_{\lambda 0}$ are the (2^λ)th-order electric multipole moments. The terms $\langle I_iK_i\lambda 0|I_fK_f\rangle$ are Clebsch-Gordan coefficients. The intrinsic electric-dipole moments used were those obtained from [13], otherwise a value of 0.075 e fm was used. The intrinsic electric quadrupole moment used was that of 6.75 e b, from the measurement of the spectroscopic quadrupole moment in Ref. [19]. The intrinsic electric-

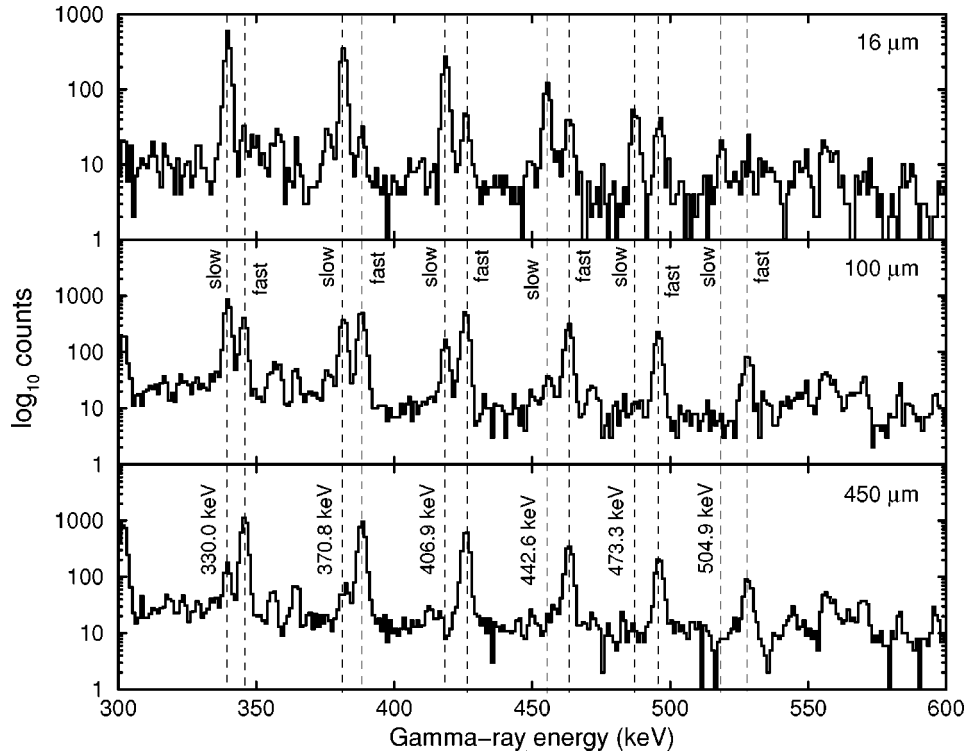

FIG. 4. Representative spectra for the recoil distances $d=16$ μm, $d=100$ μm and $d=450$ μm. The spectra were recorded by the germanium detector at 0°. The change in the relative proportion of intensity in the fully Doppler-shifted (fast) and the reduced Doppler-shifted (slow) peaks is evident. The unshifted energies are given on the lowest spectrum.

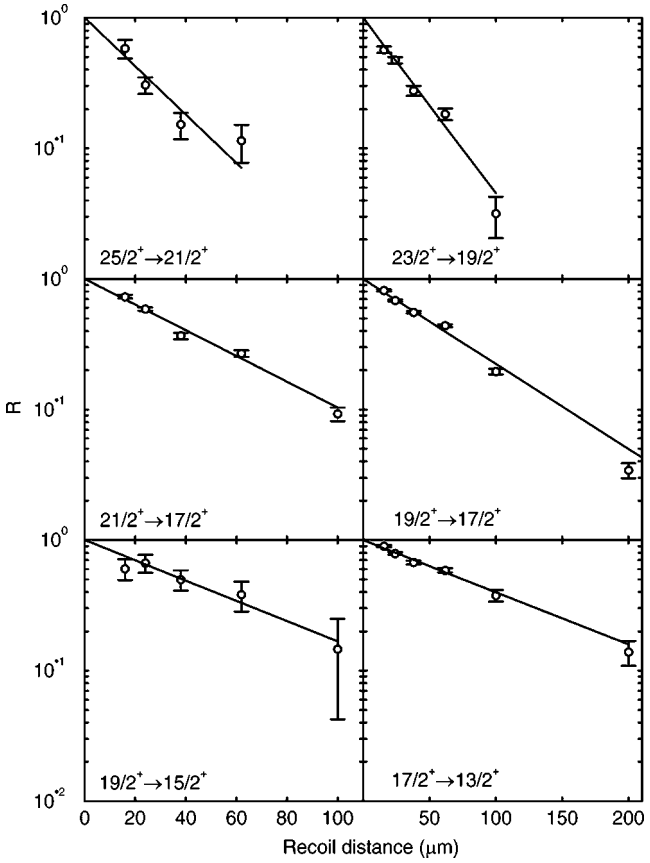

FIG. 5. Decay curves for the transitions from states in the positive-parity band. All points correspond to data corrected by the code ORACLE, as described in the text.

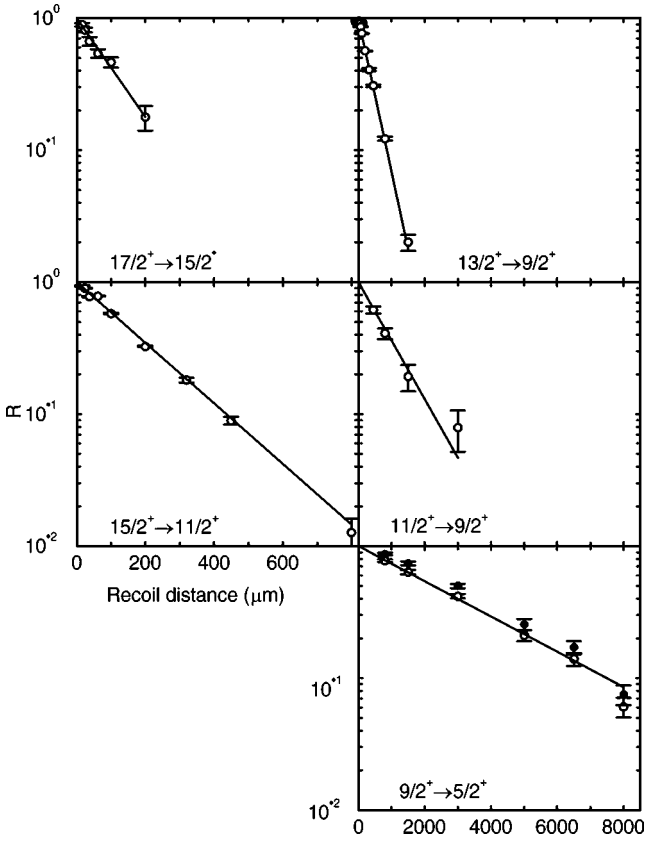

FIG. 6. Decay curves for the transitions from states in the positive-parity band. All open points correspond to data corrected by the code ORACLE, as described in the text. The solid points in the lowermost panel correspond to uncorrected data, and are shown to illustrate the effect of correcting the intensities.

octupole moment was assumed to be 1.136 $e\,\mathrm{b}^{3/2}$, equal to that of ^{150}Nd measured by Clarkson [31], and the hexadecapole matrix elements used were an average of the values of $\langle 4^+||E4||0^+\rangle$ measured for the isotonic neighbors ^{152}Sm and ^{154}Gd [32].

IV. RESULTS

The levels in the opposite-parity bands of ^{153}Eu which were populated in this work are shown in Fig. 1. In total, 33 excited states were observed, which were depopulated by about 85 gamma rays. Some gamma-ray spectra recorded by the germanium detector at 0° are given in Figs. 3 and 4. The spectra reveal the quality of the data, but also serve to illustrate the high density of gamma-ray transitions in the 100–500-keV range. With such a large number of transitions, it is not surprising that many of the transition energies are degenerate. For example there are seven transitions with energies between 150 and 160 keV, and with the recoil-distance method, many of these transitions have both a fast and slow component, which further complicates the spectra. For this reason, the gamma-ray energies used in the present work are adopted from the gamma-gamma coincidence study of Ref. [13] where it was possible to produce clean, gated spectra, from which accurate peak positions could be determined. The relative intensities of populations of the bands can be seen in Fig. 3. It should be pointed out that the $35/2^-$ state has recently been reported [33] to be isomeric, with a lifetime of 8.6(1.3) ns. If this state is isomeric, it would be expected *a priori* that Coulomb excitation would populate it only very weakly; as can been seen from Fig. 3 the 600.6-keV transition depopulating this level contains only several

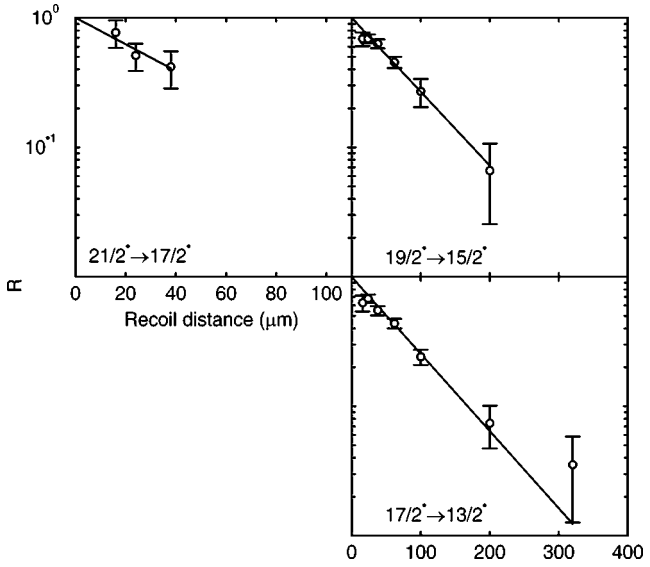

FIG. 7. Decay curves for the transitions from states in the negative-parity band. All points correspond to data corrected by the code ORACLE, as described in the text.

TABLE I. The 12 lifetime values measured in this work. For the $19/2^+$ and $17/2^+$ states it was possible to extract a lifetime from two decay branches. The weighted mean value is given for those states, and both the decay branch and the lifetime obtained for the respective branch are given in the next column to the right.

I^π	τ^{expt} (ps)		I^π	τ^{expt} (ps)
$\frac{25}{2}^+$	1.80(14)		$\frac{13}{2}^+$	28.5(7)
$\frac{23}{2}^+$	2.48(10)		$\frac{11}{2}^+$	75(5)
$\frac{21}{2}^+$	3.38(11)		$\frac{9}{2}^+$	250(8)
$\frac{19}{2}^+$	4.4(5)	$\frac{19}{2}^+ \rightarrow \frac{17}{2}^+$: 4.3(6)	$\frac{21}{2}^-$	2.7(6)
		$\frac{19}{2}^+ \rightarrow \frac{15}{2}^+$: 5.12(13)	$\frac{19}{2}^-$	6.6(6)
$\frac{17}{2}^+$	8.6(3)	$\frac{17}{2}^+ \rightarrow \frac{15}{2}^-$: 8.9(6)	$\frac{17}{2}^-$	7.2(5)
		$\frac{17}{2}^+ \rightarrow \frac{13}{2}^+$: 8.4(4)		
$\frac{15}{2}^+$	14.5(3)			

counts, suggesting that this state was not populated with any significant intensity. The effect of delayed feeding from the isomer will therefore be negligible, and need not be considered in this analysis. Indeed, no evidence for a stopped (recoil at rest) or slow (small Doppler shift) component of the 600.6-keV transition could be seen in the data.

For some contaminated transitions it was possible to measure only the fast (large Doppler shift) or slow (small Doppler shift) component, in which case the lifetime was extracted by normalizing the total intensity to that of an uncontaminated transition, because the ratio of total intensities (I_s+I_f) for any two transitions will be the same in all of the recoil-distance spectra. In total, it was possible to extract the lifetimes of 12 of the 33 excited states that were populated: nine in the positive-parity band and three in the negative-parity band. The fits made to the data by the code ORACLE are given in Figs. 5–7. The measured lifetimes are given in Table I. The errors in the lifetimes include contributions from the error in the linear fit made by the code ORACLE, in the v/c measurement, in the measurement of the recoil distance, and in the feeding correction. The latter error was estimated by varying the lifetimes of the feeding levels with lifetimes $\tau_f \pm \delta\tau_f$, between the limits $\tau_f + \delta\tau_f$ and $\tau_f - \delta\tau_f$, and investigating the subsequent effect on the lifetime under evaluation. The corrections made by ORACLE have all been tested to determine their effects on the extracted lifetimes [20]; the largest correction is found to be that due to feeding from the higher-lying states, which produced effects up to 16% in the worst cases. Variation of the deorientation parameters by 50% results in less than a 1% change in the lifetime. The correction due to radiation lost in the shifter foil is found to be about 0.1 ps. The offset in the recoil distance was found by fitting one of the strongest transitions in the positive-parity band, and was fixed for all other measurements. As an illustration of the effects of the perturbations listed in the previous section, both corrected and uncorrected R values are plotted on the lowermost panel of Fig. 6.

In order to elucidate the underlying physics, it is necessary to extract the individual $E2$, $E1$, and $M1$ matrix elements from the lifetime data. In addition to the lifetimes, this requires a knowledge of the branching ratios and mixing ratios. In principle this information was available from the experimental data. In practice, however, it was not possible to extract reliable mixing ratios for the mixed $M1/E2$ transitions although, within the large experimental errors, the data were consistent with the gamma-ray yields predicted by the Coulomb-excitation code GOSIA assuming the final set of matrix elements. Problems with contaminated transitions also meant that it was not possible to extract branching ratios for all the states. Where the branching ratio could not be measured, the values from the gamma-gamma coincidence data of Ref. [13] were adopted. The branching ratios used are given in Table II. The intensities were measured using data from the detector at 55°. The $M1$ matrix elements were extracted by assuming that the $\langle I||E2||I-1\rangle$ matrix elements were related to the $\langle I||E2||I-2\rangle$ matrix elements by the rotor relation

$$\langle I||E2||I-1\rangle^2 = \langle I||E2||I-2\rangle^2 \frac{\langle IK_i20|(I-1)K_f\rangle^2}{\langle IK_i20|(I-2)K_f\rangle^2}. \tag{6}$$

TABLE II. Measured branching ratios used in the extraction of transition probabilities and matrix elements. $\Delta\pi = y$ and $\Delta\pi = n$ indicate where there is a change in parity.

	γ-ray energy (keV)			Branching ratios			
	$\Delta I=1$	$\Delta I=2$	$\Delta I=1$	$I(\Delta I=1,\Delta\pi=y)/I(\Delta I=2,\Delta\pi=n)$		$I(\Delta I=1,\Delta\pi=n)/I(\Delta I=2,\Delta\pi=n)$	
$I_i^{\pi_i}$	$\Delta\pi=y$	$\Delta\pi=n$	$\Delta\pi=n$	Ref. [13]	This work	Ref. [13]	This work
$\frac{9}{2}^+$	41.5	193.1	109.7			0.29(2)	
$\frac{11}{2}^+$	89.4	241.8	132.1	0.025(6)		0.164(15)	
$\frac{13}{2}^+$	159.3	288.1	155.9	0.17(3)		0.145(17)	
$\frac{15}{2}^+$	177.2	330.0	174.0	0.099(6)		0.082(9)	
$\frac{17}{2}^+$	262.4	370.8	197.0	0.146(10)		0.078(6)	0.078(6)
$\frac{19}{2}^+$	236.3	406.9	210.2	0.135(7)	0.135(17)	0.055(8)	0.034(10)
$\frac{21}{2}^+$	339.6	442.6	232.5	0.105(11)	0.11(2)	0.026(8)	0.038(8)
$\frac{23}{2}^+$	272.6	473.7	241.2	0.12(5)	0.09(3)	0.05(5)	
$\frac{25}{2}^+$	393.9	504.9	263.2	0.12(2)			
$\frac{17}{2}^-$	170.3	347.9	236.2	0.20(5)		0.99(8)	
$\frac{19}{2}^-$	103.7	365.3	129.0	0.01(8)		0.16(2)	
$\frac{21}{2}^-$	201.0	437.3	308.2	0.069(12)		0.62(5)	

TABLE III. Transition probabilities, matrix elements, and moments derived from the lifetimes; Q_0 are electric quadrupole moments; D_0 are electric dipole moments. Panel (a) gives the $E2$ matrix elements derived from the $I\rightarrow(I-2)$ transitions, and (b) gives the $E1$ matrix elements.

(a) $I\rightarrow(I-2)$

I^π	$B(E2)$ $(e\,\mathrm{b})^2$	$\langle\|\|E2\|\|\rangle$ $(e\,\mathrm{fm}^2)$	Q_0 $(e\,\mathrm{b})$
$\frac{9}{2}^+$	0.60(3)	246(5)	7.79(17)
$\frac{11}{2}^+$	0.90(6)	329(11)	7.3(3)
$\frac{13}{2}^+$	0.98(3)	371(6)	6.77(11)
$\frac{15}{2}^+$	1.15(3)	428(6)	6.83(9)
$\frac{17}{2}^+$	1.09(5)	443(10)	6.38(15)
$\frac{19}{2}^+$	1.19(9)	487(18)	6.5(2)
$\frac{21}{2}^+$	1.21(5)	516(10)	6.38(12)
$\frac{23}{2}^+$	1.18(8)	533(17)	6.2(2)
$\frac{25}{2}^+$	1.22(10)	560(20)	6.2(3)
$\frac{17}{2}^-$	0.93(8)	410(17)	5.9(3)
$\frac{19}{2}^-$	1.40(13)	530(20)	7.0(3)
$\frac{21}{2}^-$	1.1(2)	480(50)	6.0(6)

(b) $I\rightarrow(I-1)$

I^π	$B(E1)$ $10^{-4}\,(e\,\mathrm{fm})$	$\langle\|\|E1\|\|\rangle$ $(e\,\mathrm{fm})$	D_0 $(e\,\mathrm{fm})$
$\frac{11}{2}^+$	2.0(5)	0.049(6)	0.048(6)
$\frac{13}{2}^+$	6.1(8)	0.093(6)	0.081(5)
$\frac{15}{2}^+$	6.15(4)	0.099(3)	0.079(3)
$\frac{17}{2}^+$	4.8(4)	0.093(4)	0.068(3)
$\frac{19}{2}^+$	10.5(15)	0.145(11)	0.100(7)
$\frac{21}{1}^+$	4.5(9)	0.099(10)	0.064(7)
$\frac{23}{2}^+$	10(3)	0.15(3)	0.094(15)
$\frac{25}{2}^+$	6.1(13)	0.126(13)	0.074(8)
$\frac{17}{2}^-$	15(4)	0.17(2)	0.121(16)
$\frac{19}{2}^-$	8(5)	0.12(4)	0.09(3)
$\frac{21}{2}^-$	11(3)	0.16(2)	0.102(14)

This model-dependent assumption allowed extraction of the $\langle I||M1||I-1\rangle$, $\langle I||E2||I-2\rangle$, and $\langle I||E1||I-1\rangle$ matrix elements for each state. The reduced matrix elements deduced from the lifetimes are given in Table III. Also given are the electric dipole moments D_0 and the electric quadrupole moments Q_0. Model-dependent $M1$ matrix elements and the (g_K-g_R) values are given in Table IV. The D_0, Q_0, and (g_K-g_R) values are plotted against spin in Fig. 8.

V. DISCUSSION

Prior to this work, the lifetimes of the $I^\pi=7/2^+$, $9/2^+$, $5/2^-$ and $7/2^-$ [16] states had been measured. The only lifetime measured in this experiment that had previously been measured was that of the $9/2^+$ state at 193.1 keV. The previously measured value of 290(20) ps differs by two standard deviations from the value from this work. The discrepancy may arise from the fact that, in Ref. [16], no mention is made of a feeding correction in extracting the lifetime. From the lifetimes and decay branching ratios, electromagnetic matrix elements and moments have been extracted. The electric quadrupole and electric dipole moments are observed to be independent of spin and parity and are scattered about mean values of 6.7(5) e b and 0.077(7) e fm, respectively.

TABLE IV. The $M1$ matrix elements deduced from the lifetimes. Use of a mixing ratio derived from a rotational model means that these values are model dependent.

$I\rightarrow(I-1)$

I^π	$B(M1)$ $10^{-1}\,(\mu_N^2)$	$\langle\|\|M1\|\|\rangle$ (μ_n)	(g_K-g_R)
$\frac{9}{2}^+$	1.0(2)	0.31(3)	0.15(2)
$\frac{11}{2}^+$	2.2(4)	0.51(4)	0.20(2)
$\frac{13}{1}^+$	3.8(6)	0.73(6)	0.25(2)
$\frac{15}{2}^+$	3.1(6)	0.70(7)	0.22(2)
$\frac{17}{2}^+$	4.2(5)	0.86(5)	0.26(2)
$\frac{19}{2}^+$	2.1(10)	0.7(2)	0.18(4)
$\frac{21}{2}^+$	3.1(9)	0.83(12)	0.22(3)
$\frac{23}{2}^+$	6(6)	1.2(6)	0.30(15)
$\frac{17}{2}^-$	23(3)	2.05(12)	0.60(4)
$\frac{19}{2}^-$	47(8)	3.1(3)	0.85(7)
$\frac{21}{2}^-$	23(5)	2.3(3)	0.59(7)

The spectroscopic quadrupole moment of the ground state has been measured to have a value of 2.41 e b [19], which corresponds to an intrinsic quadrupole moment of 6.75 e b. The values measured in this work above $11/2^+$ indicate that the value of the quadrupole moment stays constant with spin. It is difficult to explain the large values of the quadrupole moment Q_0 for the $9/2^+$ and $11/2^+$ states, which are $\sim$10–20 % larger than those of the rest of the band. The $E1$ transition connecting the $9/2^+$ and $7/2^-$ states, which would have an energy of 41.5 keV, was not reported in Ref. [13]. A

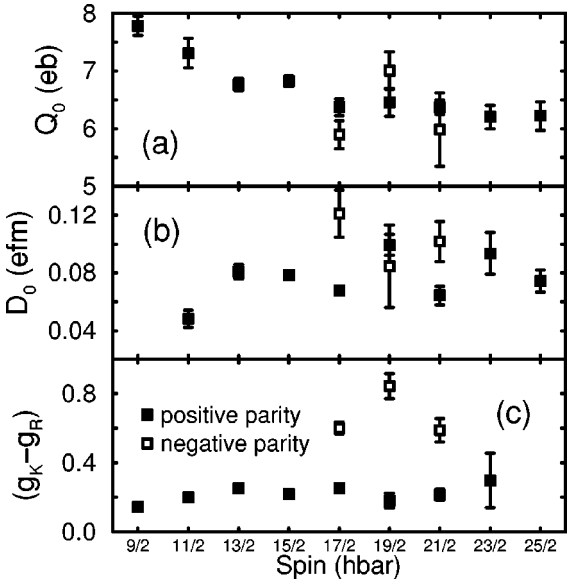

FIG. 8. Moments and g factors deduced from the lifetimes. Panel (a) shows the electric quadrupole moments Q_0 derived from the $I\rightarrow(I-2)$ transitions, (b) shows the electric dipole moments D_0, and (c) shows the (g_K-g_R) values.

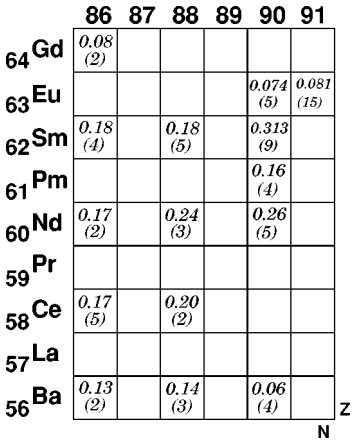

FIG. 9. Experimental values of the electric dipole moment D_0 in units of e fm. The data are taken from the compilation of Ref. [2] and references therein, apart from the ^{153}Eu value, which is extracted from these lifetime data.

transition with such low energy would be difficult to observe with the germanium detectors that were used in Ref. [13] and in this work. Assuming the same $B(E1)/B(E2)$ ratio for the $9/2^+$ state, as that measured for the $15/2^+$ state, the 41.5-keV $E1$ transition would carry a approximately 0.02 of the intensity of the 193.1-keV $9/2^+ - 5/2^+$ $E2$ transition. However, it would take an $E1$ transition with 0.5 times the intensity of the $E2$ transition in order to reduce the measured Q_0 value by $\sim$20 %. Such an intense $E1$ transition would require an abnormally large electric dipole moment for the $9/2^+$ state, and is very unlikely. Lack of knowledge about $E1$ decays or lack of knowledge about detection efficiency cannot explain the large Q_0 values for the $9/2^+$ and $11/2^+$ states.

The intrinsic dipole moments D_0 show no dependence on the spin or parity. The values are comparable in magnitude to the large collective D_0 values seen in the actinide region and some other nuclei close to ^{146}Ba, and are much larger than known $E1$ rates outside the region of strong octupole correlations. This would be expected if the $5/2^+$ and $5/2^-$ bands constitute a parity doublet. In the recent work of Ref. [13], D_0 values were deduced from $I(E1)/I(E2)$ intensity ratios, assuming a constant quadrupole moment of 6.75 e b. The D_0 values were found to show little variation and were scattered about 0.09 e fm, in fair agreement with the values measured in this work. The values for the negative-parity band, extracted from the $I^- \rightarrow (I-1)^+$ transitions, may be larger than those of the positive-parity band $[I^+ \rightarrow (I-1)^-]$, although it is difficult to draw a conclusion from only three data points. Figure 9 shows the dipole moments for a number of nuclei with $56 \leqslant Z \leqslant 64$, $86 \leqslant N \leqslant 91$ taken from the compilation of Ref. [2]. The trend shows that the electric dipole moment is a maximum for $Z \simeq 60$, $N \simeq 88$. However, it should be pointed out that shell effects make electric dipole moments an unreliable measure of octupole collectivity [34,35]. For the $N=90$ isotones it appears that the odd-proton isotopes have smaller electric dipole moments than their even-even neighbors.

The experimental characteristics of octupole deformation in an odd-Z nucleus such as ^{153}Eu would be a pair of parity-doublet bands consisting of near-degenerate states of opposite parity, interconnected by enhanced $E1$ transitions $[10^{-3}$ Weisskopf units (W.u.)]. With the bands being based on the same intrinsic parity-mixed state, the magnetic moments of the bandheads should be very nearly the same and equal to a ''hybridized'' value [4], which is intermediate between the magnetic moments of the reflection-symmetric orbitals involved. The level structure deduced in Ref. [13] and given on Fig. 1 clearly shows the distinctive pattern of a pair of parity-doublet bands. However, despite this observation, in Ref. [13] $B(M1)/B(E2)$ ratios were used to show that the bandheads have different magnetic moments, and it was concluded that the positive- and negative-parity bands arose due to the accidental degeneracy of the $[532]5/2^-$ and $[413]5/2^+$ Nilsson orbitals.

TABLE V. A comparison of magnetic moments, for the bandheads. The values from this work have been deduced using a rotational model, assuming $Q_0 = 6.75$ e b. The model predictions are calculated using a Woods-Saxon potential [35].

Magnetic moments (μ_N)	$I^\pi = \frac{5}{2}^+$	$I^\pi = \frac{5}{2}^-$
This work	1.41(5)	2.1(1)
$\mu^{\rm calc}(\beta_2=0.25,\beta_3=0)$	1.28	2.81
$\mu^{\rm calc}(\beta_2=0.25,\beta_3=0.05)$	1.67	2.40
Measured [36]	1.533(1)	3.22(23)
Reference [13] [expt. $B(M1)/B(E2)$ ratios]	1.41(14)	2.24(18)

The magnetic moments are crucial in the interpretation of parity-doublet bands. The $(g_K - g_R)$ values extracted from the present data are consistently larger in the negative-parity band than in the positive-parity band. The magnetic moments of the bandheads, calculated with weighted mean $(g_K - g_R)$ values of 0.214(8) for the $5/2^+$ band and 0.65(3) for the $5/2^-$, band are presented in Table V, in comparison to those measured and predicted elsewhere. (The value of g_R was assumed to be $Z/A=0.41$.) The model predictions ($\mu^{\rm calc}$) were calculated using a Woods-Saxon potential with the ''universal'' parameter set [37]. It is worth pointing out that the experimental magnetic moment value for the negative-parity band is smaller than that expected for the $[532]5/2^-$ orbital, which may suggest a shift towards a hybridized mean.

Recent work has presented arguments for and against the existence of parity doublets and octupole deformation in ^{153}Eu. Nosek *et al.* [38] have performed microscopic calculations and concluded that the $5/2^\pm$ states cannot constitute a parity doublet. Afanasjev and Ragnarsson [39] have satisfactorily reproduced the experimental decoupling parameters and magnetic moments without introducing reflection asymmetry. While it seems that the low-spin spectroscopic features can be explained without octupole deformation, Afanasjev and Mizutori [14] have recently examined the experimental data and concluded that octupole deformation is plausible at medium-spin values. They used rotational-frequency ratios (R) and parity-splitting (δE_π) values, as suggested by Nazarewicz and Olanders [40], and performed an analysis similar to that presented for ^{223}Th in Ref. [5]. While R and δE_π tend away from the values expected for stable octupole deformation at the highest spins, the discrepancies can be explained by the rotational alignment of a pair of neutrons. Indeed the quasiparticle alignment frequencies

are better explained in the cranked-shell-model framework when a nonzero value of β_3 is used.

VI. SUMMARY AND CONCLUSIONS

Using the recoil-distance method following Coulomb excitation of ^{153}Eu, the lifetimes of 12 excited states have been measured. The electric-quadrupole and electric-dipole moments are observed to be independent of spin and parity and are scattered about mean values of 6.7(5) *e* b and 0.077(7) *e* fm, respectively. The present measurements therefore validate the assumption made in earlier work [13], in which it was assumed that the quadrupole moments of the states in the opposite-parity bands are not appreciably different, in order to conclude that the bands have different intrinsic structures, and therefore are not a pair of parity-doublet bands. This work supports that conclusion.

The observation of the distinctive parity-doublet-type structure, together with a preponderance of $E1$ transitions and large electric-dipole moments, makes the interpretation in terms of a reflection-symmetric shape rather puzzling. If the interpretation is made in terms of reflection asymmetry, then the magnetic moments cannot be understood; similarly, a reflection-symmetric interpretation cannot explain the enhanced $E1$ transitions between the opposite-parity bands. Very little is known about octupole modes that are superimposed on nuclear ground states. It remains a challenge to the theory to explain these experimental observations. An experimental challenge would be to measure the $B(E3)$ values in ^{153}Eu using the Coulomb-excitation method which has recently been used to extract $E3$ matrix elements for some lanthanide and actinide nuclei [20,41–44]. However, a full ''Coulomb-excitation analysis'' in an odd-mass nucleus such as this will prove to be very difficult because of the large number of coupling matrix elements between the low-lying excited states.

ACKNOWLEDGMENTS

Research at the NSRL in Rochester was supported by the National Science Foundation. J.F.S. and P.M.J. acknowledge financial support from the Engineering and Physical Sciences Research Council (EPSRC). P.A.B. and G.D.J. acknowledge support from the EPSRC. A.A. and A.M.B. acknowledge support from NATO collaborative research grant number 910597.

[1] I. Ahmad and P. A. Butler, Annu. Rev. Nucl. Part. Sci. **43**, 71 (1993).
[2] P. A. Butler and W. Nazarewicz, Rev. Mod. Phys. **68**, 349 (1996).
[3] S. Ćwiok and W. Nazarewicz, Nucl. Phys. **A529**, 95 (1991).
[4] G. A. Leander and Y. S. Chen, Phys. Rev. C **37**, 2744 (1988).
[5] M. Dahlinger, E. Kankeleit, D. Habs, D. Schwalm, B. Schwartz, R. S. Simon, J. D. Burrows, and P. A. Butler, Nucl. Phys. **A484**, 337 (1988).
[6] J. R. Hughes, R. Tölle, J. De Boer, P. A. Butler, C. Günther, V. Grafen, N. Gollwitzer, V. E. Halliday, G. D. Jones, C. Lauterbach, M. Marten-Tölle, S. M. Mullins, R. J. Poynter, R. S. Simon, N. Singh, R. J. Tanner, R. Wadsworth, D. L. Watson, and C. A. White, Nucl. Phys. **A512**, 275 (1990).
[7] J. Fernandez-Niello, C. Mittag, F. Riess, E. Ruchowska, and M. Stallknecht, Nucl. Phys. **A531**, 164 (1991).
[8] N. Schulz, in *Future Directions in Nuclear Physics with 4*Π *Gamma Detection Systems of the New Generation*, edited by J. Dudek and B. Haas, AIP Conf. Proc. No. 259 (AIP, New York, 1992), p. 392.
[9] W. R. Phillips, I. Ahmad, R. Holzmann, R. V. F. Janssens, T. L. Khoo, and M. W. Drigert, Phys. Rev. Lett. **57**, 3257 (1986).
[10] W. Nazarewicz and S. L. Tabor, Phys. Rev. C **45**, 2226 (1992).
[11] W. J. Vermeer, M. K. Khan, A. S. Mowbray, J. B. Fitzgerald, J. A. Cizewski, B. J. Varley, J. L. Durell, and W. R. Phillips, Phys. Rev. C **42**, R1183 (1990).
[12] W. Urban, J. C. Bacelar, W. Gast, G. Hebbinghaus, A. Krämer-Flecken, R. M. Lieder, T. Morek, and T. Rzaca-Urban, Phys. Lett. B **247**, 238 (1990).
[13] C. J. Pearson, W. R. Phillips, J. L. Durell, B. J. Varley, W. J. Vermeer, W. Urban, and M. K. Khan, Phys. Rev. C **49**, R1239 (1994); C. J. Pearson, Ph.D. thesis, University of Manchester, 1994.
[14] A. V. Afanasjev and S. Mizutori, Z. Phys. A **353**, 267 (1995).
[15] T. Lewis and R. Graetzer, Nucl. Phys. **A162**, 145 (1970).
[16] J. E. Thun and T. R. Miller, Nucl. Phys. **A193**, 337 (1972).
[17] G. D. Dracoulis, J. R. Leigh, M. G. Slowcombe, and J. O. Newton, J. Phys. G **1**, 853 (1975).
[18] Somapriya Basu, S. Chattopadhyay, J. M. Chatterjee, R. K. Chattopadhyay, S. S. Ghurge, G. Rodrigues, R. P. Singh, S. Murulithar, and R. K. Bhowmik, Phys. Rev. C **56**, 1756 (1997).
[19] Y. Tanaka, R. M. Steffen, E. B. Shera, W. Reuter, M. V. Hoehn, and J. D. Zumbro, Phys. Rev. Lett. **51**, 1633 (1983).
[20] R. Ibbotson, B. Kotliński, D. Cline, K. G. Helmer, A. E. Kavka, A. Renalds, E. G. Vogt, P. A. Butler, C. A. White, R. Wadsworth, and D. L. Watson, Nucl. Phys. **A530**, 199 (1991).
[21] B. Kotlinski, D. Cline, A. Bäcklin, and D. Clark, Nucl. Phys. **A503**, 575 (1989).
[22] A. Renalds, B. Kotlinski, and D. Cline, NSRL Annual Report 1988, p. 185.
[23] T. K. Alexander and A. Bell, Nucl. Instrum. Methods **81**, 22 (1970).
[24] P. J. Nolan and J. F. Sharpey-Schafer, Rep. Prog. Phys. **42**, 1 (1979).
[25] D. C. Radford, Nucl. Instrum. Methods Phys. Res. A **361**, 306 (1995); **361**, 297 (1995)
[26] R. J. Sturm and M. W. Guidry, Nucl. Instrum. Methods **138**, 345 (1976).
[27] C.-Y. Wu, B. Kotlinski, D. Cline, and M. W. Simon (unpublished).
[28] R. Brenn, H. Spehl, A. Weckherlin, H. A. Doubt, and G. van Middlekoop, Z. Phys. A **281**, 219 (1977).
[29] C.-Y. Wu, Ph.D. thesis, University of Rochester, 1983; A. E. Kavka, Ph.D. thesis, University of Uppsala, 1989.
[30] T. Cozosnyka, D. Cline, and C.-Y. Wu, Bull. Am. Phys. Soc. **28**, 745 (1983); ''GOSIA Manual,'' University of Rochester (unpublished).

[31] N. Clarkson, Ph.D. thesis, University of Liverpool, 1992.
[32] H. J. Wollersheim and Th. W. Elze, Nucl. Phys. **A278**, 87 (1977).
[33] J. M. Chatterjee, Somapriya Basu-Roy, S. S. Ghugre, S. Chattopadhyay, R. P. Singh, G. O. Rodrigues, R. K. Chattpadhyay, and R. K. Bhowmik, Eur. Phys. J. A **1**, 55 (1998).
[34] P. A. Butler and W. Nazarewicz, Nucl. Phys. **A533**, 249 (1991).
[35] G. A. Leander, W. Nazarewicz, G. F. Bertsch, and J. Dudek, Nucl. Phys. **A43** , 58 (1986).
[36] M. A. Lee, Nucl. Data Sheets **37**, 487 (1982); **60**, 419 (1990).
[37] J. Dudek, Z. Szymanski, and T. Werner, Phys. Rev. C **23**, 920 (1981).
[38] D. Nosek, R. K. Sheline, P. C. Sood, and J. Kvasil, Z. Phys. A **344**, 277 (1993).
[39] A. V. Afanasjev and I. Ragnarsson, Phys. Rev. C **51**, 1259 (1995).
[40] W. Nazarewicz and P. Olanders, Nucl. Phys. **A441**, 420 (1985).
[41] R. Ibbotson, C. A. White, T. Czosnyka, P. A. Butler, N. Clarkson, D. Cline, R. A. Cunningham, M. Devlin, K. G. Helmer, T. H. Hoare, J. R. Hughes, G. D. Jones, A. E. Kavka, B. Kotlinski, R. J. Poynter, P. Regan, E. G. Vogy, R. Wadsworth, D. L. Wadsworth, D. L. Watson, and C.-Y. Wu, Phys. Rev. Lett. **71**, 1990 (1993).
[42] H. J. Wollersheim, H. Emling, H. Grein, R. Kulessa, R. S. Simon, C. Fleischmann, J. De Boer, E. Hauber, C. Lauterbach, C. Schandera, P. A. Butler, and T. Czosnyka, Nucl. Phys. **A556**, 261 (1993).
[43] C. A. White, Ph.D. thesis, University of Liverpool, 1990.
[44] R. Ibbotson, Ph.D. thesis, University of Rochester, 1995.